A Comparison of Ductility Demands on Buckling-Restrained Braces resulting from Elastic Analysis and Nonlinear Dynamic Analysis

J.D. Marshall & Z. Xie

Auburn University, Auburn, AL, USA.

B.W. Saxey

CoreBrace, West Jordan, UT, USA.

ABSTRACT:

Buckling-Restrained Braces (BRB) are becoming more popular in modern designs and retrofits of existing buildings due to their ductile, symmetric and full hysteretic characteristics. They also have the ability to be tailored for both strength and stiffness to meet specific design requirements. Analysis has shown that there may be discrepancies between the predicted ductility demand on BRBs determined from a nonlinear dynamic analysis and that determined from an equivalent lateral force method analysis. This paper will review the results of modelling of a 6-story BRBF building subjected to recorded and synthetic strong motion time histories and compare them to an elastic 2% story drift requirement from the most recent AISC seismic provisions, as well as the ductility requirements of previous AISC codes. It will also compare the resulting analysis-based overstrength factors with those resulting from the elastic analysis. The ground motions used in this study encompass near-field and far-field motions for two different seismic hazards. The research will suggest deformation ductility requirements that could be used for BRBF design and will comment on the applicability of the 2% story drift requirement in the current AISC seismic provisions.

1 INTRODUCTION

A six story structure was modelled and subjected to seismic hazards associated with LA and Riverside, California, USA. For both hazards, designs consistent with an importance of 1.0 and 1.5 were undertaken. An additional structure with a shortened yield length was modelled having the same BRB core area as the normal occupancy structure. Nonlinear analysis of models of the resulting designs were then subjected to time history motions scaled to the hazard at each site.

This paper will compare the resulting ductility demands on the BRB elements determined from nonlinear analysis to those predicted from current and past seismic steel provisions in the United States.

2 STRUCTURE DESCRIPTION

The geometry for the six story structure used for this research is based off the SAC Steel Project Joint Venture (FEMA 355C) building models. Two different locations are selected for this work, Los Angeles and Riverside, CA. The same structure geometry is used for both structures. The structure represents a typical office building adapted from the SAC model design criteria for the nine story structure and as modified by Sabelli (2001). Three different structures for each location have been generated, one Risk Category II, one Risk Category IV, and one Risk Category II structure with a shortened BRB yield length. The primary difference between the first two is the importance factor, Ie, from ASCE 7-10 (ASCE, 2010). The third structure uses the same strength requirements from the first structure but was analysed with a short yielding core length to increase the brace stiffness. The cores were shortened such that at a building story drift of 2% a core strain of approximately 3.5% resulted. The same gravity loads were used for all designs. The structures' seismic parameters are S_{DS} = 1.39g and S_{D1}=0.77g, and S_{DS} = 1.00g and S_{D1}=0.60g for the LA and Riverside locations respectively. Both

locations used Site Class D. The Riverside location resulted in Seismic Design Category D for both levels of seismic importance, while the LA location resulted in Seismic Design Category E for the I = 1.0 level of importance and Seismic Design Category F for the I = 1.5 level of importance. Table 1 contains a summary of the relevant analysis parameters for the structures at the two sites. It is interesting to note based on the fundamental period that the shortening of the yield length resulted in approximately the same stiffness change as that of the increase due to I=1.5.

Table 1 Analysis parameters for 6-story structure in LA and Riverside

Site	Importance Factor	S_{DS}	S_{D1}	SDC	T_{FDM} (s)
LA	1.00	1.39	0.77	E	1.27
LA IV	1.50	1.39	0.77	F	1.09
LA-S	1.00	1.39	0.77	E	1.10
Riv	1.00	1.00	0.60	D	1.34
Riv IV	1.50	1.00	0.60	D	1.18
Riv-S	1.00	1.00	0.60	D	1.16

The first floor height of the structure is 5.5m (18 feet) and the remaining floors all have a 4.0 m (13 foot) height. The plan dimensions including the full building envelope are 46.9 m (154 feet) by 46.9 m (154 feet), with all of the bays being 9.1 m (30 ft) square. The structure is topped with a penthouse that is 4.0 m (13 feet) high with plan dimensions of 9.1 m (30 feet) by 18.3 m (60 feet). The lateral load resisting system is comprised of six exterior bays of buckling-restrained brace frames in each direction. All of the columns are modelled with a splice at the mid-height between the third and fourth floor. Figures 1 and 2 show a plan and elevation view of the structure, respectively. The buildings were designed according to ASCE 7-10 including both strength and drift requirements using the equivalent lateral force procedure to determine the demand on the BRBs and to establish their required size.

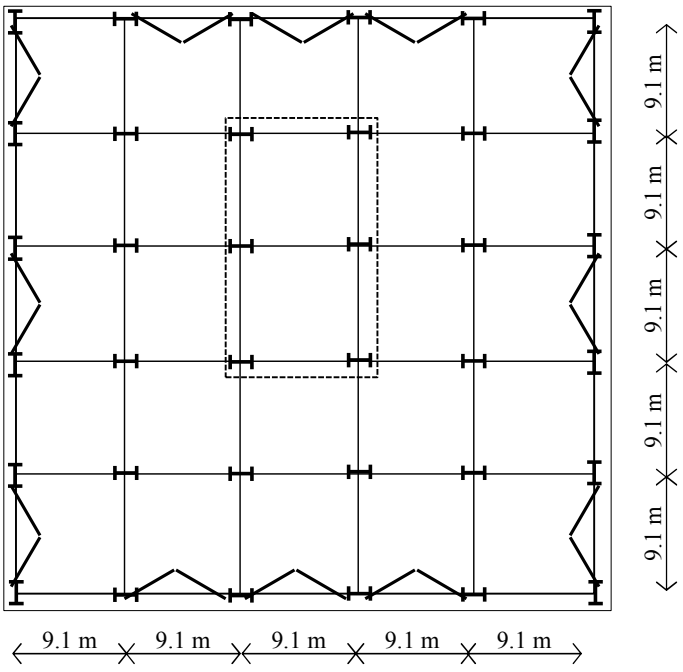

Figure 1 Plan View of Six-Story Structure (Sabelli 2001)

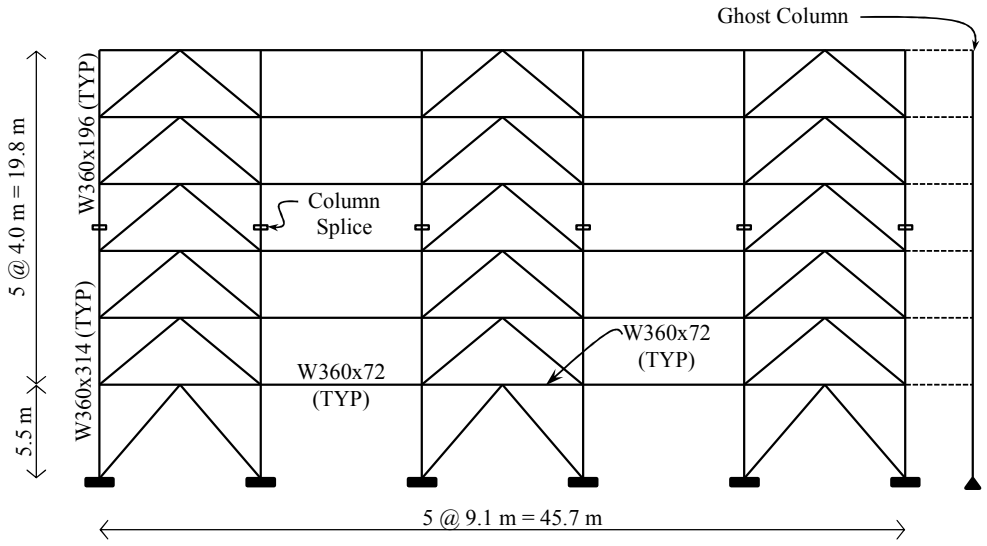

Figure 2 Elevation View of Six Story Structure

The column sizes for the gravity system were the same for the buildings in both locations as the gravity loads were all the same. The BRB forces from analysis were provided to CoreBrace, LLC. The BRBs were then sized based on a material yield stress of 262 MPa (38 ksi). The BRB sizes for all the models are provided in Table 2.

Table 2 Analysis Parameters for Six-Story Structures in LA and Riverside

Model	Story	Brace Area (mm^2)	Yield Force (kN)	Yield Length (mm)	Model	Story	Brace Area (mm^2)	Yield Force (kN)	Yield Length (mm)
LA (I=1.0)	6th	968	253.5	3706	**Riv (I=1.0)**	6th	806	211.3	3688
	5th	1290	338.1	4107		5th	1129	295.8	3716
	4th	1774	464.8	3721		4th	1452	380.3	3688
	3rd	1935	507.1	4100		3rd	1613	422.6	3680
	2nd	2097	549.4	4100		2nd	1774	464.8	3673
	1st	2258	591.6	5072		1st	1935	507.1	5017
LA IV (I=1.5)	6th	1290	338.1	4077	**Riv IV (I=1.5)**	6th	1129	295.8	3716
	5th	1774	464.8	3673		5th	1613	422.6	3680
	4th	2419	633.9	3978		4th	2097	549.4	4016
	3rd	2742	718.4	3884		3rd	2258	591.6	3995
	2nd	3065	802.9	3866		2nd	2581	676.1	3904
	1st	3226	845.2	4836		1st	2581	676.1	4884
LA-S (I=1.0)	6th	968	253.5	1725	**Riv-S (I=1.0)**	6th	806	211.3	1707
	5th	1290	338.1	1689		5th	1129	295.8	1735
	4th	1774	464.8	1692		4th	1452	380.3	1707
	3rd	1935	507.1	1697		3rd	1613	422.6	1699
	2nd	2097	549.4	1679		2nd	1774	464.8	1692
	1st	2258	591.6	1981		1st	1935	507.1	2019

3 STRUCTURE MODELLING

The structures were modelled using both SAP2000 v.15 (CSI 2013) and Perform3D v.5 (CSI 2011). Design of the structure was completed using SAP2000. All the nonlinear analysis was done with Perform 3D. Comparison of the two models was completed with modal and static analysis to verify the properties had been correctly ported into Perform 3D once the design was complete. One exterior frame was modelled including a ghost column with properties representing the weak axis strength of all the columns tributary to the frame to account for the continuous column effect. The joints in the ghost column were constrained to the adjacent frame joints. All beams were modelled such that their moments were released at the beam to column connections. All columns were modelled to have fixed bases. Any diaphragm contribution to strength and stiffness was neglected. All braces were modelled to have pinned connections at the ends of the member. The mass was distributed along the frame at the joints. Dead and live loads supported by the resisting frame were applied as a line load on the beam. The dead loads and live loads associated with the gravity framing were superimposed on the ghost column as joint loads for each floor. Inelasticity in the columns was unexpected but interacting axial-flexural hinges were assigned for the possible occurrence.

The BRBs were modelled using the BRB Compound element in Perform 3D. This element accounts for the overall stiffness of the element including the yielding core, elastic transition element and the end zone. The element also includes the hardened yield effect that has been seen in testing of BRBs. The yield stress is based on 262 MPa (38 ksi) material. The nonlinear, tri-linear model was developed based on material and brace tests completed by CoreBrace and provided as part of the brace design information. The transition from yield to hardened yield was set based on the maximum deformation. The fundamental periods of vibration from the Perform 3D models are presented in Table 1.

4 GROUND MOTION AND SCALING

Two sets of ground motions were drawn from to create the ground motion suites for the analyses. The first set drawn from was the FEMA P695 suites, both the far-field and near-field (FEMA 2009). These suites of motion are used as part of the procedure developed to quantify performance of seismic force resisting systems. Ground motions from both near and far-field sets were selected based on the spectral shape of the hazards used in the design of the buildings. A total of 20 P695 ground motions were selected with two records per motion (40 total). The same records were used for both the LA and Riverside buildings although the scaling was different for the two locations.

Amplitude scaling of the records was completed by individually scaling to the Maximum Considered Earthquake (MCE) spectrum using three points within the range of interest. The scaling was also checked to ensure that records were not scaled impractically (i.e. unrealistically large spectral acceleration or peak ground acceleration). The scaling was done such that the average spectrum from the scaled records did not fall below 90 percent of the MCE spectrum over the range of interest. The lower end of the range started at the period where at least 90 percent of the effective modal mass was included. The upper end of the range was two times the fundamental period to allow for period elongation. The end result was a range of approximately 0.3s to 3s.

The second set of ground motions, used only for the LA structure, is the SAC LA ground motions (SAC 1997). The 2 percent probability of exceedance in 50 year motions were utilized in the analyses. Due to the fact that the hazard is different than it was for the original work, the records were scaled in the same fashion as the P695 records. It should be noted that the SAC ground motion scale factors are based on scaling the records again in addition to the original scaling and modification that was applied. A total of 10 SAC ground motion records were used with two records per motion (20 total). The list of the records and associated scale factors are shown in Table 3. Figure 3 shows the individual spectra for the scaled records, the average of the scaled records and the MCE spectrum.

Table 3 FEMA P695 and SAC LA (SAC 1997) Ground Motions and Scale Factors

ID	Earthquake	Record Name	Filename	Scale Factors	
				Los Angeles	Riverside
FF01-1	Northridge, CA 1994	Beverly Hills-Mulholland	MUL009	1.44	1.04
FF01-2			MUL279	1.46	1.03
FF02-1	Northridge, CA 1994	Canyon Country-WLC	LOS000	3.45	2.47
FF02-2			LOS270	2.49	2.13
FF03-1	Duzce, Turkey 1999	Bolu	BOL000	2.05	1.64
FF03-2			BOL090	1.73	1.43
FF09-2	Kocaeli, Turkey 1999	Duzce	DZC180	3.66	2.69
FF09-2			DZC270	1.67	1.22
FF16-1	Superstition Hills, CA 1987	El Centro Imp. Co	ICC000	3.02	2.19
FF16-2			ICC000	3.65	2.45
FF18-1	Cape Mendocino, CA 1992	Rio Dell Overpass	RIO270	2.46	1.98
FF18-2			RIO360	2.13	1.72
FF19-1	Chi-Chi, Taiwan 1999	CHY101	CHY101-E	2.86	2.46
FF19-2			CHY101-N	1.77	1.49
NF02-1	Imperial Valley, CA 1979	El Centro Array #7	H-E07140	2.09	1.69
NF02-2			H-E07230	1.86	1.42
NF04-1	Superstition Hills, CA 1987	Parachute Test Site	PTS225	1.05	0.78
NF04-2			PTS315	2.37	1.66
NF06-1	Erzican, Turkey 1992	Erzican	ERZ-EW	2.18	1.70
NF06-2			ERZ-NS	1.32	0.96
NF07-1	Cape Mendocino, CA 1992	Petrolia	PET000	2.93	2.50
NF07-2			PET090	1.66	1.23
NF09-1	Northridge, CA 1994	Rinaldi Receiving Station	RRS228	0.51	0.58
NF09-2			RRS318	1.24	1.13
NF10-1	Northridge, CA 1994	Sylmar - Olive View	SYL090	1.40	1.66
NF10-2			SYL360	0.82	0.82
NF12-1	Chi-Chi, Taiwan 1999	TCU065	TCU065-E	1.02	0.75
NF12-2			TCU065-N	1.14	0.95
NF15-1	Gazli, USSR 1984	Karakyr	GAZ000	1.65	1.31
NF15-2			GAZ090	2.42	1.97
NF22-1	Cape Mendocino, CA 1992	Cape Mendocino	CPM000	1.43	1.14
NF22-2			CPM090	2.17	1.74
NF23-1	Northridge, CA 1994	LA-Sepulveda VA	0637-270	1.42	1.20
NF23-2			0637-360	1.65	1.36
NF24-1	Northridge, CA 1994	Northridge-Saticoy	STC090	3.30	1.90
NF24-2			STC180	1.53	1.28
NF26-1	Chi-Chi, Taiwan 1999	TCU067	TCU067-E	1.46	1.12
NF26-2			TCU067-N	1.80	1.34
NF27-1	Chi-Chi, Taiwan 1999	TCU084	TCU084-E	0.59	0.53
NF27-2			TCU084-N	2.06	1.49
NF28-1	Denali, AK 2002	TAPS Pump Station #10	PS10317	1.85	1.34
NF28-2			PS10047	1.23	0.92

SAC ID	Earthquake	Scale Factors
LA21	1995 Kobe	0.85
LA22		1.04
LA23	1989 Loma Prieta, CA	2.05
LA24		0.99
LA25	1994 Northridge, CA	1.02
LA26		0.88
LA27	1994 Northridge, CA	1.48
LA28		0.85
LA29	1974 Tabas, Iran	1.43
LA30		1.05
LA31	Elysian Park (Simulated)	0.91
LA32		0.85
LA33	Elysian Park (Simulated)	1.20
LA34		1.17
LA35	Elysian Park (Simulated)	1.08
LA36		0.91
LA37	Palos Verdes (Simulated)	1.10
LA38		0.93
LA39	Palos Verdes (Simulated)	1.57
LA40		1.29

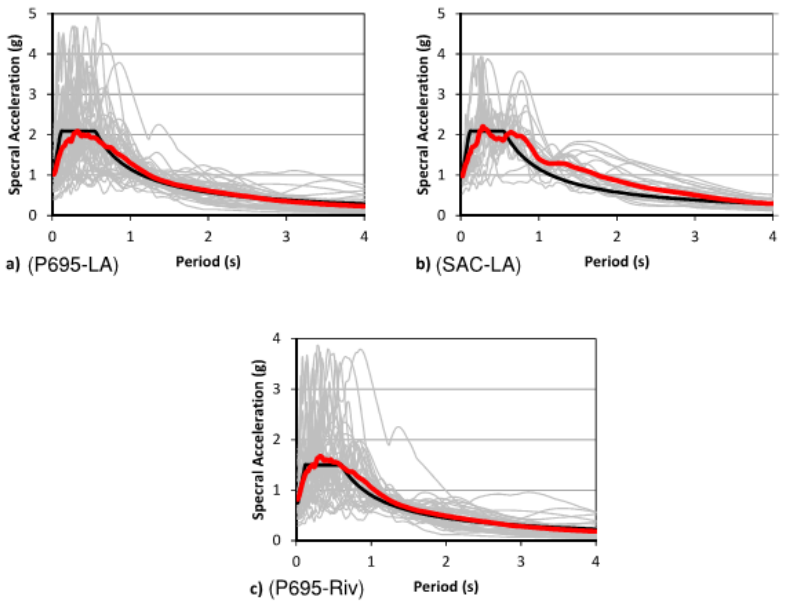

Figure 3 MCE Response Spectrum for Scaled Ground Motion Records a) P695 Records for Los Angeles b) SAC LA Records for Los Angeles c) P695 Records for Riverside

5 ANALYSIS RESULTS

The primary focus of the research is reviewing the strain and ductility demands on the buckling restrained braces. However several other response quantities are also presented to consider the overall response of the frame. It should be noted that these analyses have been carried out using MCE-level motions and as such, the limit state a code-based design should reach in this case is collapse prevention (i.e. less than 10 percent probability of collapse at MCE).

For these analyses, none of the models experienced numerical instability but some of the models did reach large drift levels. Due to the number of ground motions used, a summary of the results will be presented and discussed. The results presented show the mean, mean plus standard deviation, and maximum value for each of the response quantities so that a distribution of response can be seen. The mean value is the most important of these values in considering the ductility demands of the braces for the different structures. The maximum and residual drift values represent the maximum value at an individual story that occurred over the height of the building.

Ductility demands are presented in two forms. First, the "reference ductility demand" measured from the initial, un-elongated core state is given for both tension and compression loading over a single cycle. This measure is consistent with ductility demand limits established in codes such as AISC 341-05 (AISC 2005) and is the ductility demand associated with the reported core strain values. The second measure of ductility is the "cyclic ductility demand" which reports the largest ductility demand from the negative to the positive (or positive to negative) deformation of a cycle. For symmetrical loading, the cyclic ductility demand would be equal to 2x the reference ductility demand. Figure 4 shows a schematic representation of these two measures of ductility demand for an asymmetric loading sequence. From this figure it is clear that the cyclic ductility demand may in many cases be less than twice the maximum reference ductility demand.

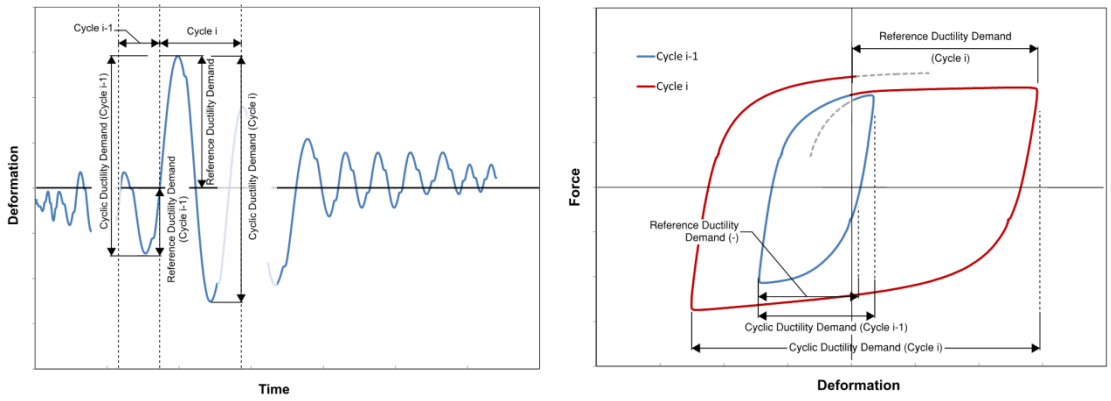

(a) (b)

Figure 4 Schematic Representation of Ductility Demand a) Deformation vs Time b) Force vs Deformation (Hysteresis) Plot

The two different brace ductility demands represent the maximum single cycle ductility demand in tension and compression. The maximum brace strain (absolute value, measured from zero) is also presented. The cumulative ductility demand is given for the brace that experienced the highest demand in the structure. The results for the Riverside and Los Angeles structures are shown in Tables 4 and 5, respectively.

Based on the results it is clear that the larger hazard results in larger ductility demands. It is also apparent that designing a building using an importance factor of 1.5 reduces the demand on the braces and the story drifts. Conversely, stiffening the structure by reducing the yielding core length resulted in considerably increased demands on the BRB. The Riverside model has a mean brace reference ductility demand of approximately 18 (not considering the shortened core length structure), indicating

that for an MCE event the maximum expected brace deformation is approximately 18 times the yield deformation (Δy). Design with an importance factor of 1.5 reduces the ductility demand by about 16%. The reduction in many other response quantities is also significant. The max story drift and the cumulative ductility demand are reduced by 27% and 25%, respectively.

Table 4 Summary of Analysis Results for Riverside Structures (FEMA P695 Records Only)

		Maximum Story Drift Ratio (Δ/h)	Maximum Story Residual Drift Ratio (Δ/h)	Maximum Column Rotation (rad)	Cyclic Ductility Demand (Tension)	Cyclic Ductility Demand (Compression)	Reference Ductility Demand (Tension)	Reference Ductility Demand (Compression)	Maximum Brace Tensile Strain (%)	Maximum Brace Compressive Strain (%)	Cumulative Ductility Demand	Max Normalized Brace Force Tension (ω)	Max Normalized Brace Force Compression (ωβ)
I_e = 1.0	**Mean**	**0.033**	**0.017**	**0.010**	**19.3**	**18.6**	**18.0**	**16.7**	**2.36%**	**2.19%**	**84.9**	**1.8**	**1.8**
	Mean +σ	0.049	0.031	0.014	29.6	28.9	26.6	24.4	3.48%	3.20%	137.4	2.1	2.1
	Max	0.081	0.061	0.020	49.4	49.6	44.2	40.9	5.80%	5.36%	303.3	2.5	2.4
	Std Dev	0.015	0.014	0.004	10.3	10.3	8.5	7.8	1.12%	1.02%	52.5	0.3	0.3
I_e = 1.5	**Mean**	**0.027**	**0.008**	**0.010**	**17.5**	**16.9**	**15.2**	**13.9**	**1.99%**	**1.82%**	**76.6**	**1.7**	**1.7**
	Mean +σ	0.037	0.014	0.012	25.3	24.9	20.8	19.0	2.73%	2.49%	120.1	1.9	1.9
	Max	0.059	0.022	0.016	45.1	44.4	33.6	29.7	4.40%	3.89%	228.9	2.6	2.5
	Std Dev	0.010	0.006	0.002	7.8	7.9	5.6	5.1	0.74%	0.67%	43.5	0.2	0.2
I_e = 1.0 Stiff	**Mean**	**0.025**	**0.005**	**0.008**	**39.8**	**39.2**	**32.1**	**30.0**	**4.21%**	**3.92%**	**185.7**	**2.4**	**2.4**
	Mean +σ	0.035	0.007	0.010	58.4	58.1	46.3	43.0	6.07%	5.64%	291.3	2.9	2.8
	Max	0.065	0.012	0.013	90.4	91.8	88.6	77.9	11.61%	10.20%	582.7	4.3	4.1
	Std Dev	0.011	0.003	0.002	18.6	18.8	14.2	13.1	1.86%	1.71%	105.7	0.5	0.5

For the LA structure a similar trend is seen. The combination of the P695 and SAC models resulted in a higher ductility demand in the structure. It should be noted that of the two suites, the SAC models had a significantly higher mean ductility demand. The mean values for the simulated SAC ground motions are significantly higher than for the remainder of the ground motions. The overall average tensile ductility demand for the normal occupancy building with normal core lengths is 21.7, while for P695 records only it is 19.5 and for the SAC records only the demand is 26.4. This is reduced by about 10% for the building in Occupancy Category IV. The two structures both show similar trends in that some performance increase is achieved using the importance factor. It also shows that the mean ductility demands can change with hazard. The stiffened design, through the shortening of the yielding core lengths, has more than twice the ductility demand, while maintaining nearly the same inter-story drift ratio as the other two designs.

A comparison of code-based ductility demands to those of Tables 4 and 5 is given in Table 6 for the mean of the Table 4 and 5 values vs the code-based predictions from AISC 341-05 (AISC, 2005) and AISC 341-10 (AISC, 2010). AISC 341-05 requires a cyclic ductility of 2xCd = 10 which, due to the symmetrical loading protocol required by the acceptance criteria, implies a required cyclic ductility demand of twice this value or 20. AISC 341-10 (2010) requires that braces have the reference ductility capacity associated with 2% story drift or that of 2xCd from the 2005 code, whichever is greater. The ductility demand associated with 2% story drift cannot be established except on a case by case basis, knowing the frame geometry and the BRB yielding core length. This calculation has been performed for the BRBs in the structure and the maximum resulting demands are given in Table 6.

From Table 6 it can be seen that while the analytical results appear to exceed the code-based requirements for the case of the synthetic SAC records, the implied code-required cyclic ductility demands (twice the reference ductility demands due to symmetrical loading protocols) are predicted fairly closely by the AISC 341-10 requirements for the I=1.0 and I=1.5 designs. The ductility demands are under predicted for the stiffened design. For the P695 records, the reference ductility demands are also very closely predicted by the AISC 341-10 code for the standard designs and the cyclic ductility demands are over predicted. The ductility demands are also fairly closely predicted or even over

predicted for the stiffened braces subjected to the P695 records. One notable exception is the reference ductility demand on the structure at the LA site where the demands are over predicted, but the cyclic ductility demands for this same structure and these records is actually under predicted.

Comparison of cyclic ductility demands from Table 6 can also be considered as applicable to the determination of overstrength. It can be noted from Figure 4(b) that the strain hardening begins once the brace has yielded even if the brace is in net compression and moving towards net tension (or vice versa). In other words, the strain hardening occurs over the entire cyclic ductility range minus the initial yielding portion and can be approximated assuming a constant rate over this range. An example of this was provided by Saxey and Daniels (2014) and gave results consistent with testing. However, testing protocols stipulated by AISC 341-10, require symmetric loading steps. As such, a test to a given ductility, say 20Δy, will have a subsequent cycle to the same negative ductility. As such, strain hardening factors for a code-required cycle of 20Δy are actually measured for a sequence with a total cyclic ductility of 40Δy. Thus, since it is shown from Table 6 that cyclic ductility is over predicted by 2x the reference ductility, the strain hardening associated with an implied cyclic ductility of 2x the reference ductility will likely over predict the actual strain hardening experienced in a real earthquake.

Table 5 Summary of Analysis Results for Los Angeles Structures

			Maximum Story Drift Ratio (Δ/h)	Maximum Story Residual Drift Ratio (Δ/h)	Maximum Column Rotation (rad)	Cyclic Ductility Demand (Tension)	Cyclic Ductility Demand (Compression)	Reference Ductility Demand (Tension)	Reference Ductility Demand (Compression)	Maximum Brace Tensile Strain (%)	Maximum Brace Compressive Strain (%)	Cumulative Ductility Demand	Max Normalized Brace Force Tension (ω)	Max Normalized Brace Force Compression (ωβ)
SAC Records	I_e = 1.0	**Mean**	**0.048**	**0.012**	**0.015**	**31.7**	**30.6**	**26.4**	**24.1**	**3.45%**	**3.16%**	**108.1**	**2.1**	**2.1**
		Mean +σ	0.068	0.020	0.019	43.3	42.3	37.1	33.9	4.86%	4.44%	138.2	2.5	2.4
		Max	0.096	0.028	0.024	54.9	53.5	52.7	47.4	6.90%	6.21%	180.7	2.9	2.7
		Std Dev	0.020	0.007	0.004	11.6	11.6	10.8	9.8	1.41%	1.29%	30.1	0.3	0.3
	I_e = 1.5	**Mean**	**0.042**	**0.012**	**0.014**	**29.8**	**28.7**	**24.3**	**21.7**	**3.18%**	**2.84%**	**96.6**	**2.1**	**2.0**
		Mean +σ	0.059	0.019	0.017	42.2	41.6	33.5	30.2	4.40%	3.96%	122.6	2.3	2.3
		Max	0.087	0.028	0.021	56.0	58.0	49.8	44.7	6.52%	5.86%	164.0	2.7	2.6
		Std Dev	0.016	0.007	0.003	12.4	12.9	9.2	8.5	1.21%	1.12%	26.0	0.3	0.3
	I_e = 1.0 Stf	**Mean**	**0.044**	**0.009**	**0.015**	**78.7**	**77.1**	**58.7**	**53.6**	**7.70%**	**7.02%**	**275.8**	**2.5**	**2.4**
		Mean +σ	0.060	0.012	0.018	107.0	105.8	81.6	74.4	10.69%	9.75%	349.9	2.9	2.8
		Max	0.084	0.015	0.022	130.0	130.4	116.0	103.5	15.20%	13.56%	460.1	3.6	3.4
		Std Dev	0.017	0.003	0.004	28.3	28.7	22.9	20.9	3.00%	2.73%	74.0	0.4	0.3
P695 Records	I_e = 1.0	**Mean**	**0.036**	**0.009**	**0.011**	**23.0**	**22.4**	**19.5**	**17.7**	**2.55%**	**2.32%**	**108.2**	**1.9**	**1.9**
		Mean +σ	0.052	0.016	0.015	35.7	35.2	28.1	25.5	3.68%	3.34%	171.1	2.2	2.2
		Max	0.083	0.027	0.018	59.4	59.0	45.5	41.5	5.96%	5.44%	318.3	2.7	2.6
		Std Dev	0.016	0.006	0.004	12.7	12.8	8.7	7.8	1.13%	1.02%	62.9	0.3	0.3
	I_e = 1.5	**Mean**	**0.031**	**0.010**	**0.010**	**20.6**	**19.9**	**17.4**	**15.6**	**2.28%**	**2.05%**	**89.7**	**1.8**	**1.8**
		Mean +σ	0.043	0.016	0.013	29.7	29.3	24.4	21.9	3.19%	2.87%	141.2	2.1	2.0
		Max	0.067	0.027	0.016	47.5	46.7	38.0	34.6	4.98%	4.53%	227.7	2.6	2.5
		Std Dev	0.012	0.006	0.003	9.1	9.4	6.9	6.3	0.91%	0.82%	51.5	0.2	0.2
	I_e = 1.0 Stf	**Mean**	**0.033**	**0.008**	**0.011**	**57.5**	**56.4**	**43.6**	**39.3**	**5.72%**	**5.15%**	**269.3**	**2.2**	**2.2**
		Mean +σ	0.047	0.013	0.014	87.7	86.7	63.2	57.0	8.28%	7.47%	427.3	2.6	2.5
		Max	0.072	0.021	0.018	149.8	147.3	98.2	88.0	12.86%	11.53%	755.1	3.3	3.2
		Std Dev	0.014	0.004	0.003	30.1	30.4	19.5	17.7	2.56%	2.32%	158.0	0.4	0.3
All Records	I_e = 1.0	**Mean**	**0.040**	**0.010**	**0.012**	**25.8**	**25.0**	**21.7**	**19.8**	**2.84%**	**2.59%**	**108.2**	**2.0**	**1.9**
		Mean +σ	0.058	0.017	0.016	38.7	38.0	31.5	28.7	4.13%	3.76%	162.4	2.3	2.3
		Max	0.096	0.028	0.024	59.4	59.0	52.7	47.4	6.90%	6.21%	318.3	2.9	2.7
		Std Dev	0.018	0.007	0.004	12.9	13.0	9.8	8.9	1.29%	1.17%	54.2	0.3	0.3
	I_e = 1.5	**Mean**	**0.034**	**0.011**	**0.012**	**23.5**	**22.8**	**19.6**	**17.6**	**2.57%**	**2.31%**	**91.9**	**1.9**	**1.9**
		Mean +σ	0.049	0.017	0.015	34.6	34.1	28.0	25.2	3.67%	3.30%	136.7	2.2	2.1
		Max	0.087	0.028	0.021	56.0	58.0	49.8	44.7	6.52%	5.86%	227.7	2.7	2.6
		Std Dev	0.015	0.006	0.003	11.1	11.3	8.3	7.6	1.09%	0.99%	44.7	0.3	0.3
	I_e = 1.0 Stf	**Mean**	**0.036**	**0.008**	**0.012**	**64.4**	**63.1**	**48.5**	**43.9**	**6.36%**	**5.75%**	**271.4**	**2.3**	**2.3**
		Mean +σ	0.052	0.012	0.016	95.3	94.2	70.2	63.7	9.20%	8.35%	407.4	2.7	2.6
		Max	0.084	0.021	0.022	149.8	147.3	116.0	103.5	15.20%	13.56%	755.1	3.6	3.4
		Std Dev	0.016	0.004	0.004	31.0	31.2	21.7	19.8	2.84%	2.59%	136.0	0.4	0.4

Table 6 Summary of Ductility Demands: Code-Based vs Analysis Based (MCE)

Site	Reference Ductility Demand				Cyclic Ductility Demand				Ductility Demand Ratio (Cyclic/Reference)		Core Strain			
	Code		Analysis		Code (Implied)		Analysis				Code		Analysis	
	AISC 341-05 (2X Cd Drift)	AISC 341-10 (2% SD)	SAC Records (Mean)	P695 Records (Mean)	AISC 341-05 (4X Cd Drift)	AISC 341-10 (2X 2% SD)	SAC Records (Mean)	P695 Records (Mean)	SAC Records	P695 Records	AISC 341-05 (2X Cd)	AISC 341-10 (2% SD)	SAC Records (Mean of Max)	P695 Records (Mean of Max)
LA	10.0	13.9	26.4	19.5	20.0	27.7	31.7	23.0	1.2	1.2	1.31%	1.81%	3.45%	2.55%
LA IV	10.0	13.9	24.3	17.4	20.0	27.7	29.8	20.6	1.2	1.2	1.31%	1.81%	3.18%	2.28%
LA Stiff	10.0	30.3	58.7	43.6	20.0	60.6	78.7	57.5	1.3	1.3	1.31%	3.97%	7.70%	5.72%
Riv	10.0	13.8	-	18.0	20.0	27.6	-	19.3	-	1.1	1.31%	1.81%	-	2.36%
Riv IV	10.0	13.8	-	15.2	20.0	27.6	-	17.5	-	1.2	1.31%	1.81%	-	1.99%
Riv Stiff	10.0	30.0	-	32.1	20.0	60.0	-	39.8	-	1.2	1.31%	3.93%	-	4.21%

Table 6 presents a ductility demand ratio which is the ratio of the maximum cyclic ductility divided by the maximum reference ductility. As stated, for symmetric loops this ductility demand ratio would be 2.0. However, it is seen in Table 6 that this ratio is 1.3 at most. Therefore, the actual strain hardening could be thought to be as low as 65% of the values indicated by testing (1.3/2.0).

Table 6 also presents a comparison of maximum core strains determined from analysis to those that would be required from a code-based analysis of AISC 341-05 and 341-10. The strains in Table 6 (as well as those in Tables 4 and 5) are determined by multiplying the ductility demands by the yield strain. The yield strain was determined as the yield stress divided by the elastic modulus (Fy/E), where the yield stress is taken as 262 MPa (38ksi). A comparison of the strains shows that the code-based strains under predict those predicted by analysis for the SAC records. It should be noted, however that the nonlinear analysis was scaled to MCE levels and as such would be expected to result in higher demands than the code-based elastic analysis. The strains resulting from the P695 records are represented fairly accurately by the AISC 341-10 predictions. These observations are consistent with the findings of the cyclic ductility demand stated earlier. So, while the strain hardening may be over predicted by current seismic provisions, levels of absolute strains measured in those code-conforming tests may under predict actual levels of strain. In fact, levels of strain nearly 1.9 times (3.45%/1.81) (again, not considering the shortened yielding core length braces) those resulting from a code-based analysis may be necessary for the brace to survive an MCE event when considering the SAC motions.

In testing of BRBs for near-fault seismic events, properly constructed BRBs were found to be able to achieve these higher levels of strain even in multiple cycles. Lanning et al. (2013) successfully tested BRBs to over 5% strain with cycles of peak-to-peak strain of over 8.5% (consistent with cyclic ductility demand of nearly 65).

6 SUMMARY AND CONCLUSIONS

The analyses presented in this paper represent a preliminary study on BRB ductility demands. The results have shown that the ductility demands at the MCE level are dependent on the seismic hazard and whether the structure is considered normal occupancy or is of higher importance and utilizes an importance factor greater than one. Current steel seismic design provisions closely predict the ductility demands on the BRB and in some cases over predict them. However, while these codes may over predict the strain hardening that a BRB will encounter in a seismic event, they may under predict the associated core strain experienced by the brace in a severe event. Additional work needs to done to further study this problem and consider other factors in BRB behaviour.

REFERENCES:

AISC (2005). ANSI/AISC 341-05 Seismic Provisions for Structural Steel Buildings. American Institute of Steel Construction, Chicago, IL.

AISC (2010). ANSI/AISC 341-10 Seismic Provisions for Structural Steel Buildings. American Institute of Steel Construction, Chicago, IL.

ASCE (2010). ASCE/SEI Standard 7 Minimum Design Loads for Buildings and Other Structures. American Society of Civil Engineers, Reston, VA.

CSI (2011). Perform-3D version 5, Computers and Structures Inc., Walnut Creek, CA.

CSI (2013). SAP 2000 version 15.2, Computers and Structures Inc., Walnut Creek, CA.

FEMA (2000). State of the Art Report on Systems Performance of Steel Moment Frames Subject to Earthquake Ground Shaking (FEMA-355C). Federal Emergency Management Agency, September 2000.

FEMA (2009). Quantification of Building Seismic Performance Factors (FEMA P695). Federal Emergency Management Agency, June 2009.

Lanning, J., Benzoni, G., Uang, C.M., (2013). The feasibility of using buckling-restrained braces for long-span bridges: Near-fault loading protocols and full-scale testing. Report No. SSRP 13/17. Dept. of Structural Engineering, Univ. of California, San Diego, La Jolla, Calif.

Sabelli, R. (2001). Research on Improving the Design and Analysis of Earthquake-Resistant Steel-Braced Frames, 2000 NEHRP Professional Fellowship in Earthquake Hazard Reduction, October 2001.

SAC (1997). Develop Suites of Time Histories. Retrieved from http://nisee.berkeley.edu/data/strong_motion/sacsteel/motions/la2in50yr.html. Accessed 7/11/2014.

Saxey, B., Daniels, M., (2014). *Characterization of Overstrength Factors for Buckling Restrained Braces.* 2014 Australasian Structural Engineering Conference, Auckland NZ